Evaluation of a commercial scintillating screen detector for proton beam QA

Abiel Ghebremedhin, Michael Taber, Gilbert Camargo, Pete Koss, Steve Ebstein[2], Baldev Patyal
Department of Radiation Medicine, Loma Linda University Medical Center, Loma Linda, CA, USA 92354
[2] Lexitek, Inc., Wellesley, MA, USA 02481

LOMA LINDA UNIVERSITY
MEDICAL CENTER

Introduction

To implement a proton beam spot scanning system in our clinic, a large detector with high spatial and temporal resolution was purchased from Lexitek, Inc. This study covers use of the detector for QA - beam quality and for collecting data for treatment planning. LLUMC proton center is planning an upgrade of one of its proton treatment nozzles to treat patients with field size as large as 40 x 40 cm using proton beam spot scanning. The spot scanning nozzle is currently installed at a research beam line and has beam spot size at iso center ranging from sigma = 2.5 mm for the highest energy to sigma = 6.5 mm at the lowest energy. A treatment planning modeling accuracy of better than 2%, requires dynamic range of 10^4 , i.e., the ratio of beam spot peak to the noise level. This work investigates the spatial resolution, light leakage, bias and background issues, pixel calibration, and shielding from non-primary radiation events.

Lexitek Detector

The detector has a thin scintillating screen, chosen among scintillators optimized for high speed, high efficiency, or low LET dependence through the Bragg peak (effectively non-quenching). It has a 16 bit scientific CCD, a fast lens, and LED illuminators for relative gain correction. The various scintillating screens are easily interchangeable. The LLUMC detector has a maximum size of 40 cm x 40 cm with micron precision mounting (Figs. 1 & 2). It comes with a MATLAB program for data analysis (single spot or multiple spots beam parameters determination) and a LabVIEW program for instrument control and collection of data. The detector comes with a grid target for spatial calibration and beam orientation determination (Fig 3) and it has optional borated poly shielding for minimizing non-primary radiation events from directly striking the CCD. Prior to any clinical use, the detector needs calibrations and background corrections to be performed.

Figure 1 – Actual image of the Lexitek detector.

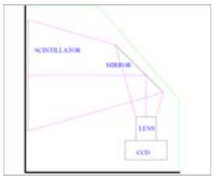

Figure 2 –Schematic of the components of the Lexitek detector.

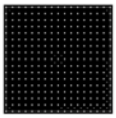

Figure 3 – Alignment grid for orientation and spatial resolution

Figure 4 – Optional borated poly shielding for the CCD

Measurements:

The following studies were made: spatial resolution and orientation study, light leakage test, bias and dark current time dependence, order of magnitude linear response, correction for gain variability, scintillator non-uniformity and vignetting from lens, shielding to radiation events and proper pixel correction from radiation events. Manufacturer supplied alignment grid target consisting of array of 5 mm circles on 25 mm center plus lines and crosses were used to check spatial resolution and orientation. Open and closed images were taken to study the effect of light leakage in a dark room. Time dependence of background was also studied. Due to limited clinical radiation field size availability, mosaic illumination was performed for relative pixel correction for a single f-stop to calibrate 40 x40 cm detector size. Using the internal LED supplied by the manufacturer, the relative vignetting effect due to the lens for different f-stops was studied. The effect of shielding supplied by the manufacturer for stopping secondary particles from directly striking CCD was also studied. The linearity of the detector response was evaluated to 0.1% of the spot peak by comparing to Exradin A16 ion chamber (0.007 ccm^3) response.

Results

Using the alignment grid target, the pixel resolution was found to be 0.47 mm/pixel and the image was oriented to give BEV display. No significant spatial distortion was observed. There is minimal effect on the detector due to light from external and internal sources (Fig. 5). The bias was about 1250 counts with small additional dark current dependent on time (Fig 6). For longer exposure, the background measurement can be performed before the actual measurement.

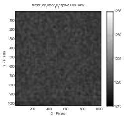

Figure 5 – Minimal light leakage from internal and external light sources .

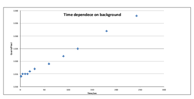

Figure 6 – Time dependence of the dark current

To correct the for scintillator non-uniformity (Fig 7), lens vignetting, and CCD pixel variability, the detector was irradiated by overlapping 16 fields (using the maximum square double-scattered beam of 15 cm^2 available in our clinic) to expose the 40 cm 40 cm detector by moving the detector around the beam (Fig. 8). An EDR film was also irradiated using the same field and the response of the film (clinically calibrated) in the high dose region was used to correct the detector response for a single f-stop of the lens (Fig 9.). To verify the correction algorithm, the same measurement was repeated and compared to the film response (Fig 10a, b). For different f-stops, the LED illuminators inside the detector were used to correct vignetting effect (Fig 11).

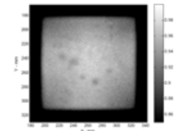

Figure 7 – detector non-uniformity due to scintillator non uniformity, vignetting and CCD pixels differences (contrast enhanced)

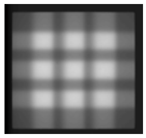

Figure 8 Mosaic calibration using actual beam

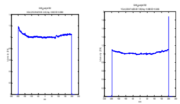

Figure 9: calibration correction factors

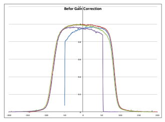

Figure 10a – individual field response before calibration shifted for comparison

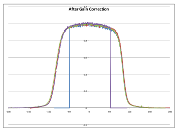

Figure 10b – individual field response after calibration shifted for comparison

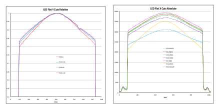

Figure 11 – Relative detector relative using LED illuminators for different lens' f-stops

For treatment planning modeling it is important that a single spot relative profile is determined to accuracy 0.01% relative to the peak dose. This is especially true when validating Monte Carlo for treatment planning modeling algorithm. To check the linearity of the detector to an order of magnitude 10^4 the detector response was compared to a micro ion chamber, A16 (0.007 cm^3). Fig 12 a, b show in linear scale and semi-log scale good agreement to .01% of the peak dose.

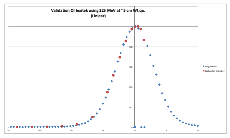

Figure 12a – Comparison of a single spot using Exradin A16 ion chamber and the Lexitek detector using a linear scale

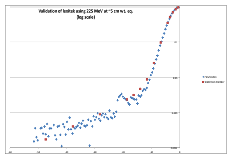

Figure 12b – Comparison of a single spot using Exradin A16 ion chamber and the Lexitek detector using a semi-log scale

The detector was irradiated to check the advantage of shielding the CCD when an exposure is made to the detector area closer to the CCD. A measurement was performed with/without shielding, using the borated phantom supplied by the manufacturer. Additional pixel correction tools were implemented, especially very useful for individual spot profiles, for removing the non-primary radiation events from registering in the CCD. Fig 13 a, b, c show the improvement of useful signal in the detector with shielding material as well as with the pixel correction algorithm implemented by the software supplied.

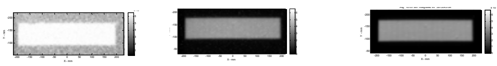

a b c

Figure 13 – Effect of shielding and analytical pixel corrections of the detector response near the CCD edge

Conclusion

The system was found to be very useful for beam quality measurements as well as a good tool for collecting data for commissioning treatment planning algorithms. The sensitivity, the resolution and the order of magnitude of the detector response is exceptionally suitable for validating beam control delivery when checking a single layer of spot scanning where the contribution of a single layer dose is very small. The system is currently being used for beam tuning as well as trouble shooting spot scanning beam delivery nozzle and helping us design out treatment planning system.

LOMA LINDA UNIVERSITY
MEDICAL CENTER